Particulate methanesulfonic acid over the central Mediterranean Sea: source region identification and relationship with phytoplankton activity

Karam Mansour[1,2,3], Stefano Decesari[1], Marco Bellacicco[4], Salvatore Marullo[4,5], Rosalia Santoleri[5], Paolo Bonasoni[1], Maria Cristina Facchini[1], Jurgita Ovadnevaite[6], Darius Ceburnis[6], Colin O'Dowd[6], Matteo Rinaldi[*,1]

[*]Corresponding author. E-mail address: m.rinaldi@isac.cnr.it (M. Rinaldi).

[1] Institute of Atmospheric Sciences and Climate, National Research Council, 40129 Bologna, Italy.

[2] Department of Physics and Astronomy, University of Bologna, 40127 Bologna, Italy.

[3] Department of Oceanography, Faculty of Science, University of Alexandria, 21511 Alexandria, Egypt.

[4] Italian National Agency for New Technologies, Energy and Sustainable Economic Development (ENEA), Frascati, Italy.

[5] Institute of Marine Sciences, National Research Council, 30122 Venezia, Italy.

[6] School of Physics, Ryan Institute's Centre for Climate & Pollution Studies, and Marine Renewable Energy Ireland, National University of Ireland Galway, University Road, Galway, H91 CF50, Ireland.

Abstract

Many efforts have been dedicated toward understanding the role of biogenic sulfur particles as a climate regulator. Herein, we investigate the relationship between the atmospheric concentration of methanesulfonic acid (MSA) and phytoplankton biomass in the Mediterranean Sea by identifying the main MSA source regions during a springtime intensive observation period. The study approach combines i) spatio-temporal correlation analysis between in situ aerosol data measured in April 2016 at Capo Granitola (southern Sicily), and high-resolution ocean color composites, ii) back-trajectory analysis, and iii) potential source contribution function (PSCF) algorithm. The southwestern Mediterranean region (between Sardinia and the Algerian coast) was identified as the most probable dimethylsulfide (DMS) source region contributing to the observed MSA concentrations. Conversely, the blooming northwestern Mediterranean Sea region did not appear to contribute significantly. The present analysis shows that the reasons may be biotic (phytoplankton type, stress level) or abiotic (sea surface temperature), or a combination of both. We also postulate that the identified source region is associated with the production of non-sea-salt-sulfate and secondary organic aerosols from the processing of sea-released volatile organic compounds.

Keywords: Mediterranean Sea, Methanesulfonic acid, Chlorophyll-a, PSCF

1. Introduction

Marine biogenic DMS emitted from the ocean can be oxidized in the atmosphere by OH, NO_3 and possibly other radical species, yielding a variety of aerosol products like MSA and sulfate (Becagli et al., 2013; Chen et al., 2018; Facchini et al., 2008; Shaw, 1983; Watts et al., 1990). MSA is one of the most important secondary organic aerosol components in the marine environment, mainly of biogenic origin (Savoie and Prospero, 1989). Together with sulfate, MSA plays a key role in the radiative properties of the atmosphere, directly through scattering solar radiation and indirectly through the formation of cloud condensation nuclei (Charlson et al., 1987; Langmann et al., 2008). A regulatory (negative) climate feedback is expected to occur if phytoplankton responds to elevated temperature and solar radiation levels by increasing their DMS production (CLAW hypothesis; Charlson et al. (1987)).

Different studies worldwide reported the seasonality of MSA and its connection to phytoplankton activity in surface seawater (Facchini et al., 2008; Li et al., 1996; Mukai et al., 1995; Yoon et al., 2007). Mukai et al. (1995) showed that the seasonal variations of MSA in the atmosphere are strongly influenced by the primary production activity around the Oki Islands in the Sea of Japan. The high MSA concentrations in the early Spring are related to the coldness of the air that enhances the deeper mixing of sea surface water and consequently increases phytoplankton blooms. Moreover, Watts et al. (1990) proposed that MSA in the North Sea and North Atlantic Ocean displays a seasonal cycle with maximum values during early summer.

The Mediterranean Sea, surrounded at its northern margin by the highly populated areas of southern Europe and at its southern margin by the African continent, is subjected to a continuous flux of anthropogenic and natural emissions from the ocean and the land. The air masses from either arid regions (Sahara Desert) or from the populated areas of the North and Eastern Europe influence the atmospheric environment above the Mediterranean. The

formation and seasonality of sulfur compounds in both gaseous and particulate phases have been extensively studied in the Mediterranean region (Bardouki et al., 2003; Kouvarakis and Mihalopoulos, 2002; Mihalopoulos et al., 2007; Mihalopoulos et al., 1997). The first measurements of aerosol sulfur species in the Eastern Mediterranean (Crete island) reported that the contribution of biogenic sulfate was between 0.6% and 28.3% with the highest values during summer (Mihalopoulos et al., 1997). Kocak et al. (2004) measured 610 daily aerosol samples on the northeastern Mediterranean coast of Turkey, covering four years (1996-1999) to define the chemical composition of aerosol and its potential source regions. They showed that the MSA displays a seasonal variability, ranging from 0.02±0.03 μg m^{-3} in wet winter (November-February) to 0.05±0.05 μg m^{-3} in dry summer (June-September). In the Western Mediterranean, two intensive campaigns in the summers of 2009 and 2010 (Schembari et al., 2014) and one campaign in summer 2011 (Bove et al., 2016) were carried out, reporting MSA concentrations of the order of 54±28 ng m^{-3}. These works quantified the biogenic sulfate contribution, based on MSA concentrations, to be more important (26%) than that from dust and sea salt. Becagli et al. (2013) elucidated the relationship between MSA and phytoplankton activity in the central Mediterranean Sea, evidencing a clear anti-correlation between atmospheric MSA and surface chlorophyll-a concentration on a multi-annual scale. They proposed that the production of DMS in the marine surface layer is mainly related to the phytoplankton physiology so that in the summer season, high irradiance and shallow depths in the upper mixed layer lead to enhanced DMS emissions and accordingly high MSA concentrations in the atmosphere.

The production of dimethylsulfoniopropionate (DMSP), the biochemical precursor of DMS, depends not only on the different phytoplankton classes (Keller et al., 1989; Orellana et al., 2011), but also on the physiological state of the cells within each group (Becagli et al., 2013; Matrai and Vernet, 1997). Furthermore, DMS release in the water column is highly related to

phytoplankton senescence rather than growth (Kwint and Kramer, 1995; Laroche et al., 1999; Zhuang et al., 2011) which means that healthy and exponentially growing cells release little amounts of DMSP. Toole and Siegel (2004) suggested that the net biological production and concentration of DMS in the upper mixed layer is directly proportional to the ultraviolet radiation dose at the surface and to seasonally varying variables such as sea surface temperature (SST) and solar flux. This assumption is supported by Becagli et al. (2013) and Vallina and Simo (2007) who showed a strong correlation between DMS concentrations and the solar radiation dose in the upper mixed layer of the open ocean regardless of latitude, phytoplankton biomass and temperature. In the Eastern Mediterranean atmosphere, the monthly DMS measurements showed a seasonal variability that is highly correlated to SST (Kouvarakis and Mihalopoulos, 2002).

The present study aims at investigating the relationship between marine biological activity and the production of biogenic aerosol in the Central Mediterranean Sea by identifying the source regions of MSA observed at a semi-remote coastal location. The surface chlorophyll-a concentration (CHL) is chosen as the reference surrogate for tracing the evaluation of marine biological activity (Yoon et al., 2007) because it is the most widely available and validated ocean color parameter. Moreover, in a previous approach, Rinaldi et al. (2013) concluded that there is no need to substitute CHL with other biological surrogates, which are generally affected by larger and less quantified uncertainties, considering that they do not produce better results than CHL in tracing marine aerosol properties.

The paper is organized as follows; in Section 2, we present the in situ and satellite data measurements and describe the procedure of the PSCF algorithm. In Section 3, the results of merging satellite with in situ MSA data and of the trajectory-based source location effort are shown. The discussion is in Section 4 while conclusions are drawn in Section 5.

2. Data and Methods

2.1 In situ aerosol measurements

The aerosol characterization campaign was carried out between 07 and 25 April 2016, at the I-AMICA Capo Granitola (CGR) Climate Observatory (37.66670° N, 12.65000° E; 5ma.s.l.), located 12 Km to the South-East from Mazara del Vallo (Cristofanelli et al., 2017) and facing the Sicily Channel. Further description of the campaign can be found in Rinaldi et al. (2019).

The atmospheric concentration of submicron MSA was measured online by an Aerodyne High Resolution- Time of Flight- Aerosol Mass Spectrometer (HR-ToF-AMS) (DeCarlo et al., 2006). The HR-ToF-AMS was operated according to the recommendations by Jimenez et al. (2003), Allan et al. (2003) and Canagaratna et al. (2007). Briefly, the measurements were performed by alternating between "V" and "W" ion path modes every 2.5 min. The concentrations reported here correspond to the data collected in V mode. The resolving power of the V-ion mode was about 2000-2200 during the whole campaign. Ionization efficiency (IE) calibrations were performed at the beginning, in the middle and after the campaign. Filter blank acquisitions during the campaign were performed once a day, at randomly chosen moments, to evaluate the background and correct for the gas-phase contribution. All data were analyzed using the standard ToF-AMS analysis software SQUIRREL v1.51 and PIKA v1.10 (D. Sueper, available at: http://cires.colorado.edu/jimenez-group/ToFAMSResources/ToFSoftware/index.html) within Igor Pro 6.2.1 (WaveMetrics, Lake Oswego, OR).

The mass spectrometer was connected to the station main aerosol sampling system (Cristofanelli et al., 2018) and the aerosol was dried to about 40% RH by means of a Nafion drier before sampling. The HR-ToF-AMS collection efficiency (CE) was calculated based on aerosol composition, according to Middlebrook et al. (2012).

The MSA concentration was derived from the concentration of mass fragment $CH_3SO_2^+$, following the procedure by Ovadnevaite et al. (2014). Since the MSA quantification method has not been standardized in the AMS, and its fragmentation pattern could be instrument dependent (Zorn et al., 2008), the obtained concentrations were validated against offline measurements. MSA concentration was determined by ion chromatography analysis of PM1 filter samples (24 hours time-resolution) collected in parallel to the mass spectrometry measurements (Rinaldi et al., 2019). As presented in Fig. S1 (supporting material), the online method agreed quite well with the offline MSA filter measurements and any discrepancy was within instrument uncertainties. In this work, we have chosen to use online MSA data, instead of the more standard offline ones, as the former provides a higher time-resolution during the campaign. The high time-resolution of online data allowed a better comparison with air mass back trajectories, in particular, for the PSCF approach.

2.2 Ocean color data

Level-4 satellite chlorophyll-a concentration (CHL; mg m^{-3}) data at 1 km spatial resolution over the Mediterranean Sea were downloaded from the EU Copernicus Marine Environment Monitoring Service (CMEMS; http://marine.copernicus.eu/). The CHL fields (OCEANCOLOUR_MED_CHL_L4_NRT_OBSERVATIONS_009_041) were estimated by the application of the Mediterranean Ocean Color 4 bands (MedOC4) algorithm (D'Alimonte et al., 2003; Volpe et al., 2007). For a detailed description of the product can be found at http://marine.copernicus.eu/documents/PUM/CMEMS-OC-PUM-009-ALL.pdf and http://marine.copernicus.eu/documents/QUID/CMEMS-OC-QUID-009-038to045-071-073-078-079-095-096.pdf.

A second satellite parameter used in this study is the optical particulate backscattering at 443 nm (b_{bp}) wavelength. The $b_{bp}(443)$ data over the Mediterranean Sea, as generated by the ocean color component of the European Space Agency Climate Change Initiative project (ESA-

CCI; available at: https://www.oceancolour.org/), is available with daily composites of merged sensors (*i.e.* MERIS, MODIS Aqua, SeaWiFS LAC & GAC, VIIRS) and a spatial resolution roughly 4.63 km. The b_{bp} is obtained by the application of the Quasi Analytical Algorithm (QAA; Lee et al. (2002) and Lee (2014)). The accuracy of the QAA was demonstrated by Melin et al. (2005), Melin et al. (2011), Brewin et al. (2015), Pitarch et al. (2016) and Bellacicco et al. (2016).

2.3 Phytoplankton Carbon estimation

The daily phytoplankton carbon biomass (PHYC) data are computed using the equation of Behrenfeld et al. (2005) based on the light backscattering coefficient in seawater due to particles, b_{bp} (λ) as:

$$\boldsymbol{PHYC = [b_{bp}(443) - b_{bp}NAP(443)] \times SF} \qquad \textbf{[mg C m}^{-3}\textbf{]},$$

where $b_{bp}(443)$ is the particulate backscattering coefficient (m^{-1}) at 443 nm and it is used as a measure of the particle concentration in seawater (Dall'Olmo et al., 2012; Dall'Olmo et al., 2009; Westberry et al., 2008; Westberry et al., 2010). The $b_{bp}NAP(443)$ is the background contribution of non-algal particles to $b_{bp}(443)$ and it is equal to the constant value of 0.00035 m^{-1}, following Behrenfeld et al. (2005). This constant background value was estimated as the intercept of the least-square linear regression fit between CHL and b_{bp} by using global SeaWiFS monthly ocean color data (1997–2002). The $b_{bp}NAP$ represents a global estimate of b_{bp} by the stable heterotrophic and detrital components of the surface particle population. The scaling factor ($SF = 13000$ mg C m^{-2}) is a constant to convert b_{bp} (m^{-1}) into $PHYC$ (Behrenfeld et al., 2005; Bellacicco et al., 2018; Bellacicco et al., 2016; Westberry et al., 2008) which is consistent with field estimates from different oceanic regions.

2.4 Potential source contribution function

The Potential Source Contribution Function (PSCF) is used widely to identify probable source areas of observed aerosol chemical components (Chang et al., 2011; Dall'Osto et al., 2017; Karaca et al., 2009; Polissar et al., 2001). It combines the back trajectories (BTs) information with the measured data to produce probability fields for potential source regions.

In this study, five-days back trajectories (HYSPLIT4 with GDAS data; available at: https://ready.arl.noaa.gov/HYSPLIT.php) (Rolph et al., 2017; Stein et al., 2015) were calculated four times (00, 06, 12 and 18 hour) a day during the sampling period from 07 to 25 April 2016, with arrival position at the sampling station, 100 m above the mean sea level. The MSA data were averaged over 6 hours periods (3 hours before and after the arrival time of each back trajectory) to associate with MSA concentration value at each trajectory.

The Mediterranean Sea was divided into 1°×1° latitude/longitude grid cells. The conditional probability that the air passing through the $\boldsymbol{ij}$-th cell have a high MSA concentration when arriving to CGR is given by:

$$\boldsymbol{PSCF_{ij} = (m_{ij}/n_{ij}) \times W_{ij}}$$

Where $\boldsymbol{n_{ij}}$ is the number of trajectories with segment endpoints in a cell $\boldsymbol{ij}$ and $\boldsymbol{m_{ij}}$ is the subclass ($\boldsymbol{m_{ij} < n_{ij}}$) of trajectories connected to MSA concentrations above a threshold defining high concentrations that in this case are the median and third quartile of the MSA concentration distribution. Only cells with at least 7 segment endpoints or more are used and the PSCF values were multiplied by a weighting factor as indicated below, to downscale the contribution of cells with a low number of endpoints.

$$\boldsymbol{W_{ij} = 1}, \quad \text{if } \boldsymbol{n_{ij} \geq 50}$$

$$\boldsymbol{W_{ij} = 0.8} \quad \text{if } \boldsymbol{7 \leq n_{ij} < 50}$$

$$W_{ij} = 0, \qquad \text{if } n_{ij} < 7$$

3. Results

The daily pattern of MSA concentration measured at CGR during the campaign, obtained from 5-minutes time resolution AMS measurements, is presented in Fig. 1. The mean (± standard deviation) and median of MSA for the entire study period were 0.04±0.02 and 0.033 μg m^{-3}, respectively. The highest MSA concentration was observed on 16 April, while generally, the first and last parts of the campaign were characterized by lower concentrations. The above concentration levels are consistent with those reported by Kouvarakis and Mihalopoulos (2002) and Kocak et al. (2004), for Eastern Mediterranean sites, and within the range of variability for the April month presented by Becagli et al. (2013), for MSA in the Sicilian Channel.

In the following paragraphs, we will investigate the source regions of the MSA measured at CGR, within the Mediterranean Basin, with the aim of shedding light on the relationship between marine biological activity and secondary organic aerosol production. This will be done by following a multi-step approach.

3.1 MSA space and time correlation with CHL

One step of our approach is based on spatio-temporal correlation analysis between atmospheric MSA and sea surface CHL concentrations. The basic assumption is that marine biogenic organic aerosol (here represented by MSA) should follow the evolution of marine biological activity (traced by CHL), as previously observed for the North Atlantic Ocean (Rinaldi et al., 2013). For this reason, we looked for sea regions, within the Mediterranean domain, characterized by a positive and significant correlation between in situ measured MSA and surface CHL. In our interpretation, these regions have a higher probability of being related to the MSA concentrations observed at the sampling site.

Becagli et al. (2013) reported an inverse relationship between monthly CHL and MSA concentrations around Lampedusa Island (Sicily Channel), in the central Mediterranean Sea, studying four years of observations (2005-2008). A similar inverse relationship between DMS and CHL is reported by Toole and Siegel (2004) in the Sargasso Sea and by Vallina and Simo (2007) in the northwestern coastal Mediterranean Sea. These findings are not in contradiction with our hypothesis: the anti-correlation between monthly CHL and MSA (Becagli et al., 2013) was observed in long time scales (multi-years) and it is clearly driven by the different seasonality of the two correlated variables. On long time scales (6 months to multi-year) changes in nutrients, light, SST, etc... induce physiological changes in the phytoplankton (so-called photoacclimation, which is particularly strong in the Mediterranean Sea (Bellacicco et al., 2016)) that may modify the relation between CHL concentration and DMS emission. This means that the same value of surface CHL concentration, in two different seasons, can be associated with significantly different DMS fluxes to the atmosphere, making CHL unsuitable as a tracer on the long term. On sub-monthly time scales, as in this experiment, the variability of oceanic physical parameters is minimized and DMS emissions are primarily modulated by biological productivity. Consequently, we assume that MSA atmospheric concentrations can be traced back to variations in CHL in the sea.

Rinaldi et al. (2013) and O'Dowd et al. (2015) showed that the correlation between marine aerosol properties and satellite tracers of oceanic biological activity is maximized when an appropriate time-lag is considered. The time-lag was attributed, in that case, to the time scale of the processes responsible for the production and release of organic matter that could be transferred within sea-spray. Similar results were obtained by Lee et al. (2015) and Wang et al. (2015), who observed a delay time (4 to 10 days) between changes in sea-spray chemical composition and CHL peaks in controlled laboratory experiments. Also, McCluskey et al. (2017) demonstrated 4-days time-lag between ice nucleating particles (INPs) activation in sea

spray aerosol and CHL concentration peaks, with the same experimental setup. Based on the above findings, the effect of different time-lags (between zero and 25 days) on the spatial distribution of the MSA vs CHL correlation was tested. This was done by shifting back in time the considered time window along the CHL time-series of "n" days to obtain the "Lag = n" map (Rinaldi et al., 2013).

The correlation coefficients between MSA atmospheric concentration (daily averages) at CGR and satellite-derived ocean color data, at each grid point covering the Mediterranean Sea domain, were computed to obtain the correlation maps presented in Fig. 2. A standard least squares regression was used for this purpose.

The spatial distributions of the correlation coefficient (R), resulting from the regression analysis between MSA concentration (μg m^{-3}) measured at CGR and CHL surface water concentration (mg m^{-3}) for two specific time-lags, are shown in Fig. 2 (full set of maps with all the tested time-lags are presented in Fig. S2). In the maps, the colors represent only positive and significant correlation coefficients. The analysis of the correlation maps obtained with different time-lags between CHL and MSA shows that the maximum correlation is found at two regions in the Western Mediterranean with different time delays. These regions are consistently located upwind to the sampling point with respect to the main wind direction during the measurement period, as shown by the back-trajectory analysis (Fig. S3). The two regions are potentially the main sources of DMS that is converted to the MSA observed at CGR during April 2016.

The first region, in the Southwestern Mediterranean (blue box, hereafter denoted as Region 1), comprises the area between 37°−39° N and 02°−10° E and shows a maximum correlation at a time-lag of 8 days. About 43% of the pixels within this region show a positive and significant correlation (Fig. 3b). In the second region (Northwestern Mediterranean: 40°−44.5° N and 03°−10° E; red box, hereafter denoted as Region 2), the best correlation occurred at 16 days

time-lag with approximately the same percentage of significant positive pixels at Region 1. The significantly negative pixels within both regions are very low, approximately 4%, indicating an overall significant positive correlation.

The correlation coefficient frequency distributions over both regions separately (Fig. 3c and 3d) for time-lags of 0, 8, and 16 days clearly show the increase in the correlation between CHL and MSA as a function of the considered delay time. The correlation between MSA and CHL over Region 1 increases toward positive correlation from the peak at R=0.45 up to nearly R=0.95 at time-lag 8 days. While in Region 2, both amplitude and peak distribution value increases as the time-lag is increased from 0 to 16 days.

In our interpretation, the time-lag between CHL and MSA represents the time scale of the biological processes responsible for the production of DMS in the seawater, together with the physico-chemical processes leading to the atmospheric formation of MSA from DMS. This latter can be estimated in 1-2 days (Barnes et al., 2006; Boucher et al., 2003; Hezel et al., 2011; Kloster et al., 2006). Indeed, it is known from the literature that the release of DMSP (precursor of DMS) is limited for healthy and exponentially growing cells, while high quantities of DMSP are released by stressed or senescent cells (Laroche et al., 1999; Zhuang et al., 2011) and by phytoplankton subjected to grazing (Wolfe and Steinke, 1996) or infected by viruses (Hill et al., 1998). All these processes occur at a later stage than the exponential growth phase and can contribute to the observed time-lag between the CHL time series and in situ measured aerosol properties. A related point to consider is that the average travel time from the two selected regions to the sampling point is of the order of one day, based on the back-trajectory analysis. Therefore, aerosol transport alone, nor DMS oxidation time, cannot explain the observed delay between the CHL and MSA time series.

The scatter plots between the average CHL (the mean value of all cells) in the maximum correlation areas (Region 1 and Region 2) and MSA are shown in Fig. S4. Further discussion about the robustness of the CHL-MSA relationship can be also found in the supporting material.

3.2 Potential source contribution function

The high time-resolution MSA data were combined with air-mass back trajectories following the PSCF method (Chang et al., 2011). PSCF allows a geographical source attribution for high-resolution aerosol data, showing the pixels associated with the highest concentrations (defined in this work as above the median and the third quartile), that correspond to the probable source regions. In other words, PSCF provides another way of assessing MSA sources over the Mediterranean basin for the investigated period, alternative to and completely independent from the statistical analysis presented in the previous Section.

We point out here that PSCF was run by considering 5-days back trajectories, which is a time frame adequate to track air mass transport across the Mediterranean basin, as demonstrated by Fig. S3. This five-days time frame is not related to the lag time considered in the "MSA vs CHL" correlation analysis. As already addressed, in the regression analysis, the lag time serves to phase the CHL time series with the MSA one. In other words, the lag time in the correlation approach refers mainly to processes occurring before the formation of MSA from its precursor DMS, while the five days considered in the PSCF approach regard the transport of MSA (after its formation) to the receptor point.

The analysis (Fig. 4) showed that the most probable homogeneous source region for the measured MSA was the southwestern Mediterranean Sea, along with some spots around Sicily, mainly due to coastal production. When looking at concentrations above the third quartile (Fig. 4b), source areas tend to concentrate over the sea region between Sardinia and the Algerian coast, which corresponds to Region 1. This result confirms that Region1 is likely the most

important source area of MSA observed at CGR during the campaign, while Region 2 is not confirmed as a source region by PSCF.

The altitude of the BTs passing over Regions 1 and 2 was analyzed, in order to asses if this can explain the discrepancy of results between PSCF and CHL correlation analysis regarding Region 2. Indeed, BTs over Region 2 tend to pass at a higher altitude compared to Region 1 (40% of BTs pass lower than 1000 m over Region 2, compared to 78% over Region 1; more details can be found in Fig. S3 and its caption), even though low-passing BTs are not negligible in Region 2. The PSCF run only on low BTs (< 500 m height) shows that most of the BT endpoints in Region 2 do not ever associate with MSA concentrations above the median (Fig. S6), strongly suggesting that Region 2 was not a hotspot for MSA production during the campaign.

3.3 MSA space and time correlation with PHYC

Although CHL concentration is the most widespread proxy of the algal biomass concentration in seawater, its retrieval does not take into account the physiological adjustments that phytoplankton undergoes in response to changes in light and nutrient conditions (Bellacicco et al., 2016; Halsey and Jones, 2015), leading to potential biases in the estimation of the biomass trends. For this reason, Behrenfeld et al. (2005) developed an alternative algal biomass concentration index, in terms of total phytoplankton carbon (PHYC).

PHYC data over the Mediterranean Sea were combined with MSA data at CGR, following the same approach as for CHL data, to check if a different proxy for algal activity could lead to different results. It is worth highlighting that here we use the PHYC-MSA correlation only in a qualitative sense, to compare with the above results, as the low quality of PHYC data is a limiting factor in studying its relationship with MSA. The estimation of PHYC biomass and its

physiological status with a high resolution from space has remained so far an elusive target (Behrenfeld et al., 2005; Bellacicco et al., 2016).

A significant correlation between PHYC and MSA has been found, with time-lag about 6-9 days, mainly over Region 1, as shown in Fig. 5. These results support those obtained by CHL-MSA correlation maps and PSCF algorithm, which point to Region 1 as potentially the main source of MSA observed at CGR during the Spring campaign.

Despite the results of Becagli et al. (2013), which showed a better correlation between the P^B index (ratio of algal Carbon and Chlorophyll) and MSA than CHL vs. MSA, the corresponding derived phytoplankton physiology index PHYC:CHL ratio, from satellite data, does not show a significant correlation with MSA in this study, in the correlation map approach (not shown). We cannot, however, exclude that, with future improvements in ocean color remote sensing and algorithm development, PHYC and PHYC:CHL ratio may become a better surrogate of algal activity in this kind of approach.

4. Discussion

The results of the combined approach (spatio-temporal correlation analysis, BT analysis and PSCF) point to the southwestern Mediterranean Sea, particularly the region between Sardinia and the Algerian coast, as the most likely source of MSA measured at CGR during April 2016. This source is at a greater distance upwind the Sicilian Channel than previously estimated (Becagli et al., 2013). Considering that a significant fraction of aerosol MSA can be found in the sub-micrometer size range (Rinaldi et al., 2010; Watts et al., 1990), long-range transport of MSA within the Mediterranean basin is clearly possible. The removal of MSA from the atmosphere is carried out mainly through wet and/or dry deposition with a lifetime estimated to be about one week (Gondwe et al., 2003; Hezel et al., 2011).

The role of Region 2 as MSA source, evidenced by the correlation with CHL, is clearly not supported by the PSCF approach nor by the correlation with PHYC. Interestingly, Region 2, roughly corresponding to the Gulf of Lion–Ligurian Sea region, is considered the most biologically productive region of the Mediterranean Sea (Fig. S7), away from coasts and river discharge (D'Ortenzio and d'Alcala, 2009; Salgado-Hernanz et al., 2019; Volpe et al., 2012; Volpe et al., 2007) and it is characterized by an intense phytoplankton bloom in springtime (Fig. S8). In order to assess the reasons why this highly biologically productive region is not contributing significantly to the MSA atmospheric burden as observed at the sampling location, reanalysis meteorology data (ERA5; (C3S, 2017)) were analyzed to evidence the main differences between Region 1 and Region2. The daily mean time series (Fig. S9) of wind speed (WS), sea surface temperature (SST), net surface solar radiation (SSR) and relative humidity (RH) in Region 1 and Region 2 show that all the parameters are basically identical between the two regions, with the exception of SST. On the time scale of our study, a positive and significant correlation is found between MSA concentration and SST (together with SSR and RH; Table 1). This agrees with the fact that warmer SST leads to enhanced phytoplankton growth and consequently enhances DMS emission (Kim et al., 2018). In addition, warmer SST may enhance the degassing of DMS to the atmosphere. Indeed, the difference in SST could explain why Region 1 emits significant amounts of DMS (acting as MSA source) while Region 2 does not. This would also suggest that Region 2 may become more important for the Mediterranean aerosol MSA budget later on in the summer when SST increases at higher latitudes.

The significant correlation observed between MSA concentration and net surface solar radiation is in line with previous observations by Toole and Siegel (2004), Becagli et al. (2013) and Vallina and Simo (2007) who showed a strong positive correlation between DMS and the solar radiation dose in the upper mixed layer of the open ocean. Nevertheless, given the lack of

significant differences in this parameter between the two Regions, SSR cannot explain the difference in DMS/MSA production.

Apart from physical (abiotic) parameters, the different DMS/MSA productivity of the two considered regions may be due also to differences in the biological communities and biochemical conditions characterizing the two marine areas. There is plenty of evidence in the recent literature that the Mediterranean Sea can be divided into different bioregions (Basterretxea et al., 2018; D'Ortenzio and d'Alcala, 2009; Lavigne et al., 2013; Navarro et al., 2014; Salgado-Hernanz et al., 2019; Sammartino et al., 2015) characterized by different CHL seasonality, phytoplankton population and ecological succession. The analysis performed by Basterretxea et al. (2018), based on neural network classification of 17 years of ocean color data, clearly shows that Regions 1 and 2 belong to different bioregions, with consequent diversity in the phytoplankton community composition. Based on the monthly maps of phytoplankton functional type distribution over the Mediterranean Sea by El Hourany et al. (2019), during April, the dominant phytoplankton functional type is Synechococcus, with a minor contribution from Haptophytes in Region 1 and Diatoms in Region 2. The DMSP content of phytoplankton cells, related to DMS emissions from the sea surface after DMSP excretion and processing, differs markedly between different phytoplankton types (Gali et al., 2013; Keller et al., 1989; McParland and Levine, 2019) and may also vary significantly depending on the stress level. The above evidence suggests a possible biotic reason at the base of the observed diversity in DMS/MSA production between the two considered sea regions.

5. Conclusions

A combined approach based on spatio-temporal correlation analysis, back trajectory analysis and PSCF has been carried out on the Mediterranean Sea domain to investigate the relationship between marine biological activity and biogenic aerosol production in springtime. In situ

aerosol MSA data along with high spatial-resolution (1 km) satellite ocean color data were used for this purpose.

In detail, the implemented approach indicates that the marine region with the highest probability of being the source of MSA measured at CGR, during Spring 2016, is located roughly between 37 and 39 °N and between 02 and 10 °E (southwestern Mediterranean Sea, between Sardinia and the Algerian coast). This source region is located further upwind than previously assumed for MSA measured in the Sicily Channel area.

The identified source area does not coincide with the most biologically productive sea area during the measurement period, which is located across the Ligurian Sea and Gulf of Lion. The reasons why the blooming North Western portion of the Mediterranean Sea is not contributing significantly to the aerosol burden observed at CGR may be biotic (different phytoplankton types or stress conditions) or abiotic factors (SST), which may also be intertwined in determining the observed effect.

Although it has been demonstrated that the yearly cycle of the marine biological activity as observed by CHL measurements in the Mediterranean Sea is not in phase with the atmospheric concentration of aerosol MSA, the present work shows that a relationship between phytoplankton activity and MSA concentration can be evidenced, on short time scales.

This work shows that the combined approach introduced here can be used to investigate the production of reactive gases and aerosols, in relation to marine biological activity, in the Mediterranean Sea on a sub-seasonal time scale. Achieving a better characterization of the time and space relationships linking marine biological activity to atmospheric composition can significantly improve the current prediction capability of the atmosphere evolution in a changing climate, both on regional and global scales.

The source region identified in the present study is probably also associated to the production of non-sea-salt-sulfate, which shares the same precursor and formation routes with MSA and, possibly, of secondary organic aerosols from the processing of volatile organic compounds released from the sea surface. However, concentrations of other trace species are certainly influenced by anthropogenic emissions, leaving MSA as the only tracer measured at CGR suitable to perform spatial source attribution analysis.

Acknowledgements

This work was funded by FP7-ENV-2013, Project BACCHUS (grant n. 603445). The Capo Granitola Observatory was set up in the framework of the I-AMICA Project (Italian National Operation Program for Research and Competitiveness 2007–2013), while the station operations and QA/QC actions in the period 2014–2018 were supported by the Project of National Interest Next data (funded by MIUR) and the H2020 ACTRIS-2 Project. The April 2016 field campaign was conducted as part of Air-Sea-Lab (CNR Joint Lab project). Francescopiero Calzolari and Maurizio Busetto are greatly acknowledged for technical support during the campaign. M. Bellacicco has a postdoctoral fellowship by the European Space Agency (ESA) in the context of the ESA Living Planet Fellowship Project PHYSIOGLOB: Assessing the interannual physiological response of phytoplankton to global warming using long-term satellite observations, 2018–2020. A special thanks to the ESA Ocean Color-Climate Change Initiative (ESA OC-CCI) team for providing free access to the data time series (http://www.esaoceancolour-cci.org) and the Copernicus climate change service (C3S) for providing ERA5 reanalysis meteorological data.

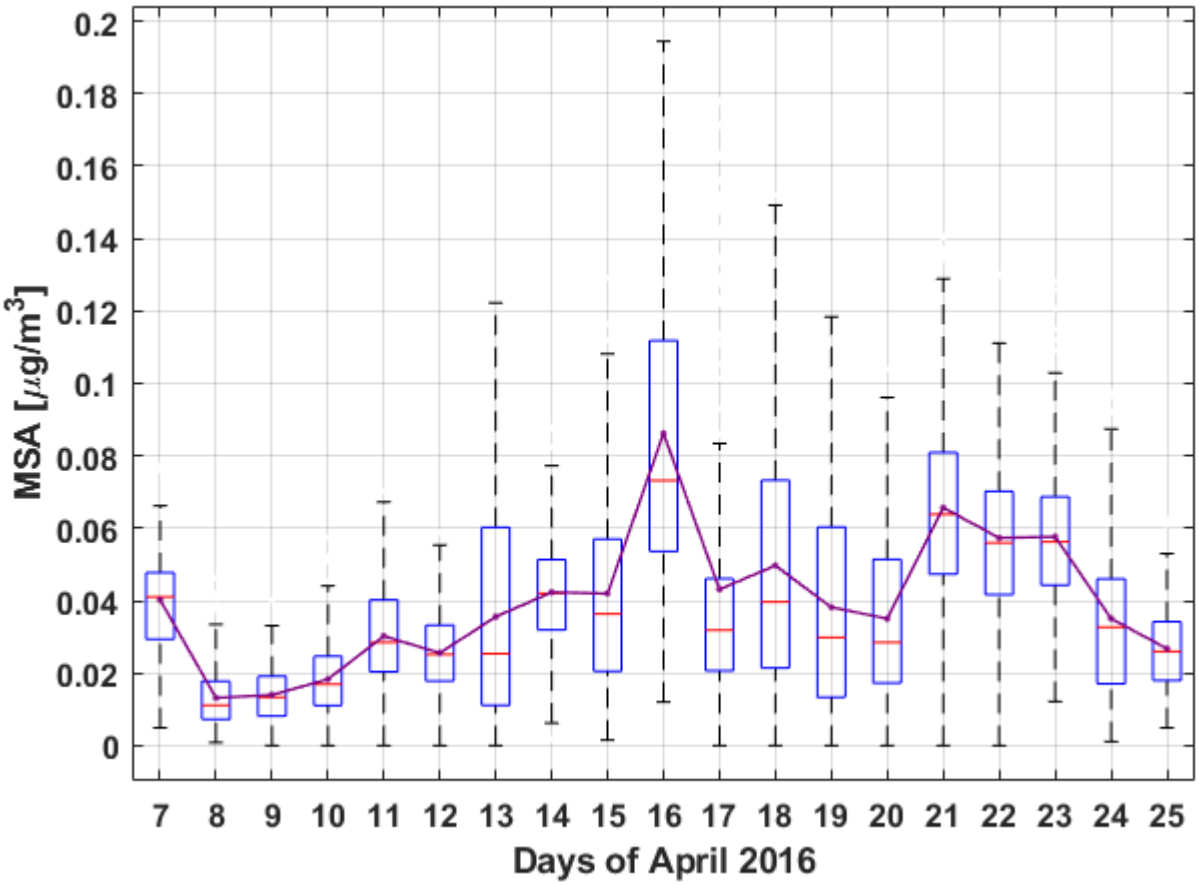

Fig. 1: Daily Pattern of MSA atmospheric concentration at CGR during 07-25 April 2016. On each box that represents a day, the central mark indicates the median, and the bottom and top edges of the box indicate the 25th and 75th percentiles, respectively. The whiskers extend to the minimum and maximum data points. The dark purple line represents the daily mean.

ss

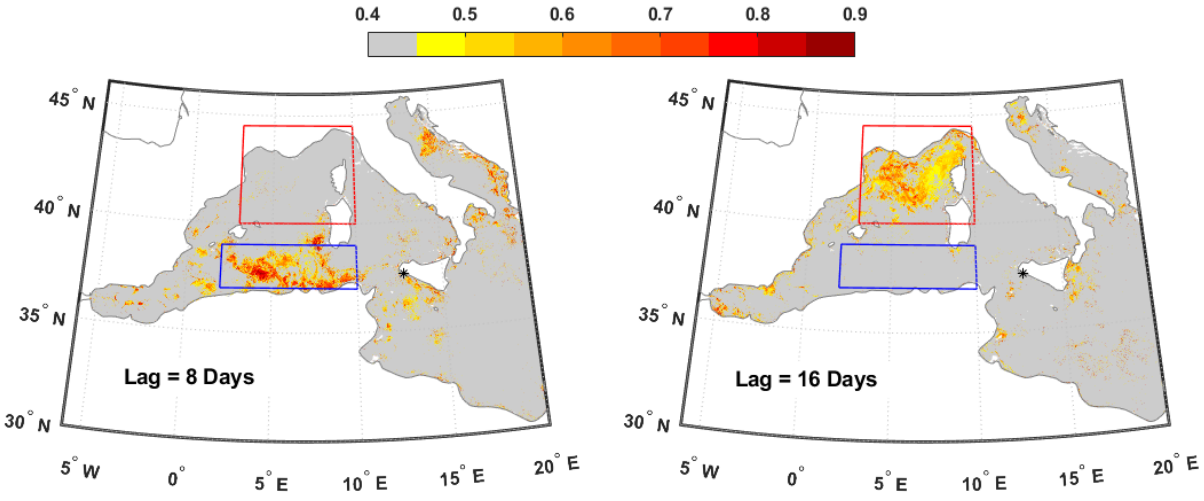

Fig. 2: Spatial distribution of the correlation coefficient between MSA at CGR and CHL over the Mediterranean Sea for 8 days time-lag (left) and for 16 days time-lag (right). The grey color represents negative and non-significant correlation coefficients at 95% confidence level. The black star corresponds to CGR station. The blue box area comprises grid coordinates 37°−39° N and 02°−10° E (Region 1) while the red box area comprises grid coordinates 40°−44.5° N and 03°−10° E (Region 2). These boxes indicate the area selected to compute the curves presented in Fig. 3 and the regression lines reported in Fig. S4.

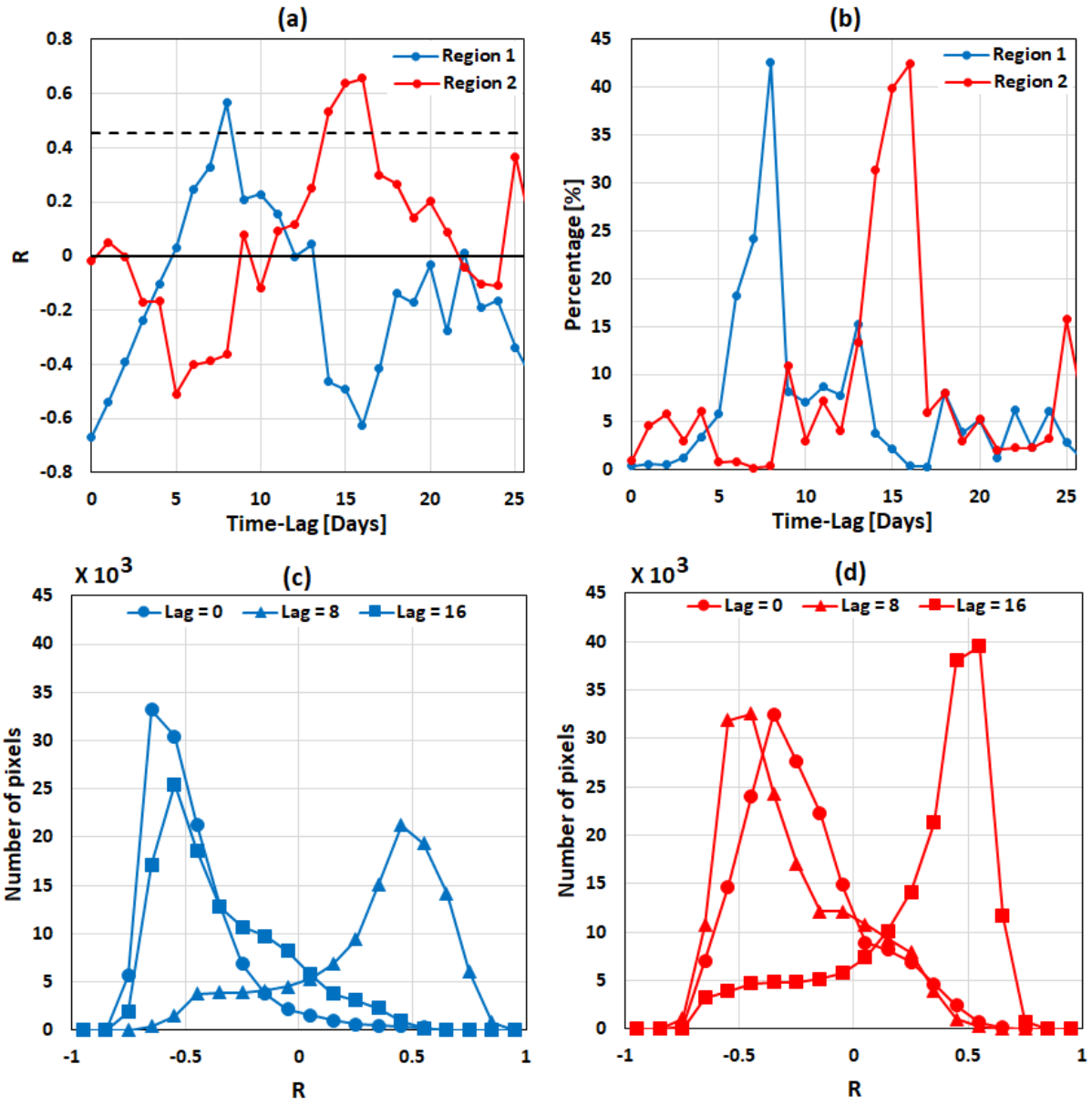

Fig. 3: a) Correlation coefficient between CHL and MSA as a function of the time-lag, the black dashed line represent the critical level of significant correlation at 95% confidence limit; b) percentage of the number of pixels with positive and significant correlation in regions of interest; c) and d) correlation coefficient frequency distribution at areas of interest for time-lags of 0, 8, and 16 days.

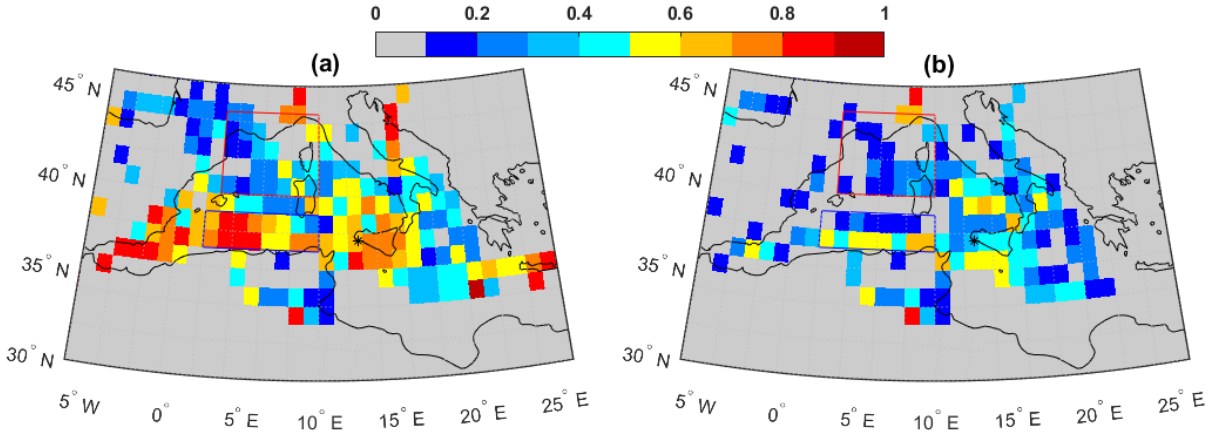

Fig. 4: Potential source contribution function plots for MSA over the period 07th-25th April 2016. The source of high MSA concentrations is defined as above the median (left) and the third quartile (right). The color scale represents the probability from 0 to 1.

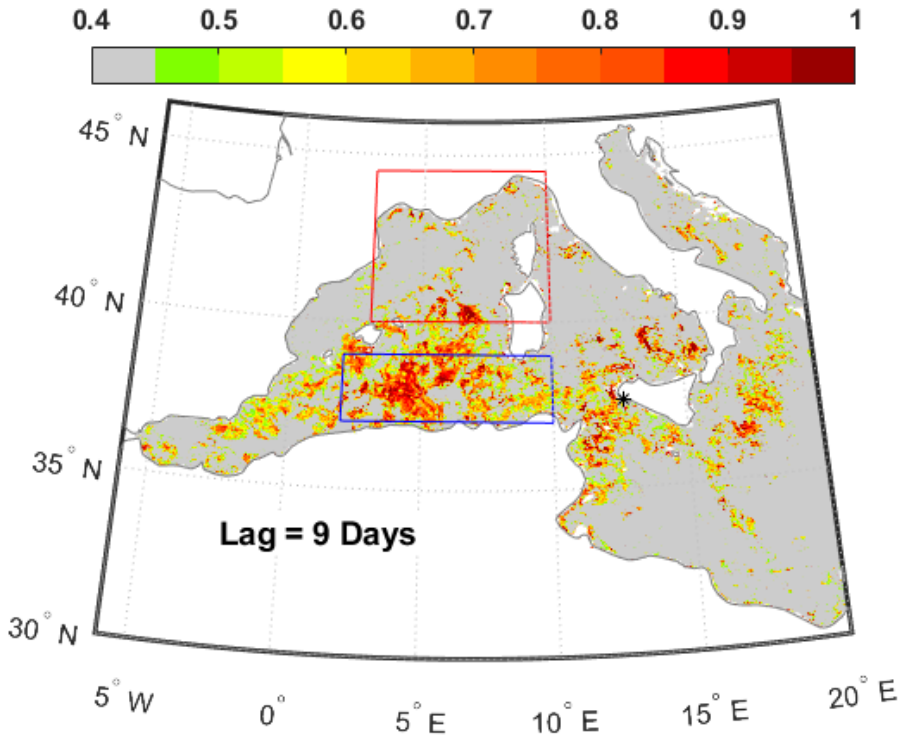

Fig. 5: Spatial distribution of the correlation coefficient between MSA at CGR and PHYC over the Mediterranean Sea for 9-days time-lag. The grey color represents negative and non-significant correlation coefficients at 95% confidence level. Regions 1 (blue box) and 2 (red box), as well as CGR station (black-star) are shown.

Table 1: Daily correlation coefficients between MSA measured at CGR and the atmospheric components over the interesting regions in the Mediterranean Sea. *Rc* is the critical correlation coefficient and *n* is the number of samples. *represents non-significant values at 95% confidence level. The meteorological data are extracted from global ERA5 with spatial resolution 0.25×0.25°.

	Samples Number	WS	SST	SSR	RH	CHL
Region 1	***Daily***	-0.28*	0.6	0.64	0.52	0.56
Region 2	***n*=19; Rc=0.45**	-0.51	0.67	0.58	0.36	0.66

References

Allan, J.D. *et al.*, Quantitative sampling using an Aerodyne aerosol mass spectrometer - 1. Techniques of data interpretation and error analysis, *Journal of Geophysical Research-Atmospheres* **108**(2003).

Bardouki, H. *et al.*, Gaseous (DMS, MSA, SO2, H2SO4 and DMSO) and particulate (sulfate and methanesulfonate) sulfur species over the northeastern coast of Crete, *Atmospheric Chemistry and Physics* **3**(2003), pp. 1871-1886.

Barnes, I., Hjorth, J., Mihalopoulos, N., Dimethyl sulfide and dimethyl sulfoxide and their oxidation in the atmosphere, *Chemical Reviews* **106**(2006), pp. 940-975.

Basterretxea, G., Font-Munoz, J.S., Salgado-Hernanz, P.M., Arrieta, J., Hernandez-Carrasco, I., Patterns of chlorophyll interannual variability in Mediterranean biogeographical regions, *Remote Sensing of Environment* **215**(2018), pp. 7-17.

Becagli, S. *et al.*, Relationship between methanesulfonate (MS-) in atmospheric particulate and remotely sensed phytoplankton activity in oligo-mesotrophic central Mediterranean Sea, *Atmospheric Environment* **79**(2013), pp. 681-688.

Behrenfeld, M.J., Boss, E., Siegel, D.A., Shea, D.M., Carbon-based ocean productivity and phytoplankton physiology from space, *Global Biogeochemical Cycles* **19**(2005).

Bellacicco, M. *et al.*, Global Distribution of Non-algal Particles From Ocean Color Data and Implications for Phytoplankton Biomass Detection, *Geophysical Research Letters* **45**(2018), pp. 7672-7682.

Bellacicco, M., Volpe, G., Colella, S., Pitarch, J., Santoleri, R., Influence of photoacclimation on the phytoplankton seasonal cycle in the Mediterranean Sea as seen by satellite, *Remote Sensing of Environment* **184**(2016), pp. 595-604.

Boucher, O. *et al.*, DMS atmospheric concentrations and sulphate aerosol indirect radiative forcing: a sensitivity study to the DMS source representation and oxidation, *Atmospheric Chemistry and Physics* **3**(2003), pp. 49-65.

Bove, M.C. *et al.*, PM10 source apportionment applying PMF and chemical tracer analysis to ship-borne measurements in the Western Mediterranean, *Atmospheric Environment* **125**(2016), pp. 140-151.

Brewin, R.J.W. *et al.*, The Ocean Colour Climate Change Initiative: III. A round-robin comparison on in-water bio-optical algorithms, *Remote Sensing of Environment* **162**(2015), pp. 271-294.

C3S, C.C.C.S., ERA5: Fifth generation of ECMWF atmospheric reanalyses of the global climate . Copernicus Climate Change Service Climate Data Store (CDS), d*ate of access* . https://cds.climate.copernicus.eu/cdsapp#!/home. (2017).

Canagaratna, M.R. *et al.*, Chemical and microphysical characterization of ambient aerosols with the aerodyne aerosol mass spectrometer, *Mass Spectrometry Reviews* **26**(2007), pp. 185-222.

Chang, R.Y.W. *et al.*, Aerosol composition and sources in the central Arctic Ocean during ASCOS, *Atmospheric Chemistry and Physics* **11**(2011), pp. 10619-10636.

Charlson, R.J., Lovelock, J.E., Andreae, M.O., Warren, S.G., OCEANIC PHYTOPLANKTON, ATMOSPHERIC SULFUR, CLOUD ALBEDO AND CLIMATE, *Nature* **326**(1987), pp. 655-661.

Chen, Q.J., Sherwen, T., Evans, M., Alexander, B., DMS oxidation and sulfur aerosol formation in the marine troposphere: a focus on reactive halogen and multiphase chemistry, *Atmospheric Chemistry and Physics* **18**(2018), pp. 13617-13637.

Cristofanelli, P. *et al.*, Investigation of reactive gases and methane variability in the coastal boundary layer of the central Mediterranean basin, *Elementa-Science of the Anthropocene* **5**(2017), pp. 1-21.

Cristofanelli, P. *et al.*, New "Smart" Systems for Atmospheric Aerosol and Reactive Gas Sampling in Ambient Air, *Sensors* **18**(2018).

D'Alimonte, D., Melin, F., Zibordi, G., Berthon, J.F., Use of the novelty detection technique to identify the range of applicability of empirical ocean color algorithms, *Ieee Transactions on Geoscience and Remote Sensing* **41**(2003), pp. 2833-2843.

D'Ortenzio, F., d'Alcala, M.R., On the trophic regimes of the Mediterranean Sea: a satellite analysis, *Biogeosciences* **6**(2009), pp. 139-148.

Dall'Olmo, G., Boss, E., Behrenfeld, M.J., Westberry, T.K., Particulate optical scattering coefficients along an Atlantic Meridional Transect, *Optics Express* **20**(2012), pp. 21532-21551.

Dall'Olmo, G., Westberry, T.K., Behrenfeld, M.J., Boss, E., Slade, W.H., Significant contribution of large particles to optical backscattering in the open ocean, *Biogeosciences* **6**(2009), pp. 947-967.

Dall'Osto, M. *et al.*, Antarctic sea ice region as a source of biogenic organic nitrogen in aerosols, *Scientific Reports* **7**(2017).

DeCarlo, P.F. *et al.*, Field-deployable, high-resolution, time-of-flight aerosol mass spectrometer, *Analytical Chemistry* **78**(2006), pp. 8281-8289.

El Hourany, R. *et al.*, Phytoplankton Diversity in the Mediterranean Sea From Satellite Data Using Self-Organizing Maps. Journal of Geophysical Research: Oceans (2019).

Facchini, M.C. *et al.*, Important Source of Marine Secondary Organic Aerosol from Biogenic Amines, *Environmental Science & Technology* **42**(2008), pp. 9116-9121.

Gali, M. *et al.*, Diel patterns of oceanic dimethylsulfide (DMS) cycling: Microbial and physical drivers, *Global Biogeochemical Cycles* **27**(2013), pp. 620-636.

Gondwe, M., Krol, M., Gieskes, W., Klaassen, W., de Baar, H., The contribution of ocean-leaving DMS to the global atmospheric burdens of DMS, MSA, SO2, and NSS SO4=, *Global Biogeochemical Cycles* **17**(2003).

Halsey, K.H., Jones, B.M., Phytoplankton Strategies for Photosynthetic Energy Allocation, *Annual Review of Marine Science, Vol 7* **7**(2015), pp. 265-297.

Hezel, P.J. *et al.*, Modeled methanesulfonic acid (MSA) deposition in Antarctica and its relationship to sea ice, *Journal of Geophysical Research-Atmospheres* **116**(2011).

Hill, R.W., White, B.A., Cottrell, M.T., Dacey, J.W.H., Virus-mediated total release of dimethylsulfoniopropionate from marine phytoplankton: a potential climate process, *Aquatic Microbial Ecology* **14**(1998), pp. 1-6.

Jimenez, J.L. *et al.*, Ambient aerosol sampling using the Aerodyne Aerosol Mass Spectrometer, *Journal of Geophysical Research-Atmospheres* **108**(2003).

Karaca, F., Anil, I., Alagha, O., Long-range potential source contributions of episodic aerosol events to PM10 profile of a megacity, *Atmospheric Environment* **43**(2009), pp. 5713-5722.

Keller, M.D., Bellows, W.K., Guillard, R.R.L., DIMETHYL SULFIDE PRODUCTION IN MARINE-PHYTOPLANKTON, *Acs Symposium Series* **393**(1989), pp. 167-182.

Kim, A.H., Yum, S.S., Lee, H., Chang, D.Y., Shim, S., Polar Cooling Effect Due to Increase of Phytoplankton and Dimethyl-Sulfide Emission, *Atmosphere* **9**(2018).

Kloster, S. *et al.*, DMS cycle in the marine ocean-atmosphere system - a global model study, *Biogeosciences* **3**(2006), pp. 29-51.

Kocak, M., Kubilay, N., Mihalopoulos, N., Ionic composition of lower tropospheric aerosols at a Northeastern Mediterranean site: implications regarding sources and long-range transport, *Atmospheric Environment* **38**(2004), pp. 2067-2077.

Kouvarakis, G., Mihalopoulos, N., Seasonal variation of dimethylsulfide in the gas phase and of methanesulfonate and non-sea-salt sulfate in the aerosols phase in the Eastern Mediterranean atmosphere, *Atmospheric Environment* **36**(2002), pp. 929-938.

Kwint, R.L.J., Kramer, K.J.M., DIMETHYLSULFIDE PRODUCTION BY PLANKTON COMMUNITIES, *Marine Ecology Progress Series* **121**(1995), pp. 227-237.

Langmann, B., Scannell, C., O'Dowd, C., New Directions: Organic matter contribution to marine aerosols and cloud condensation nuclei, *Atmospheric Environment* **42**(2008), pp. 7821-7822.

Laroche, D. *et al.*, DMSP synthesis and exudation in phytoplankton: a modeling approach, *Marine Ecology Progress Series* **180**(1999), pp. 37-49.

Lavigne, H. *et al.*, Enhancing the comprehension of mixed layer depth control on the Mediterranean phytoplankton phenology, *Journal of Geophysical Research-Oceans* **118**(2013), pp. 3416-3430.

Lee, C. *et al.*, Advancing Model Systems for Fundamental Laboratory Studies of Sea Spray Aerosol Using the Microbial Loop, *Journal of Physical Chemistry A* **119**(2015), pp. 8860-8870.

Lee, Z., Update of the Quasi-Analytical Algorithm (QAA_v6) http://www.ioccg.org/groups/Software_OCA/QAA_v6_2014209.pdf. (2014).

Lee, Z.P., Carder, K.L., Arnone, R.A., Deriving inherent optical properties from water color: a multiband quasi-analytical algorithm for optically deep waters, *Applied Optics* **41**(2002), pp. 5755-5772.

Li, S.M., Barrie, L.A., Toom, D., Seasonal variations of methanesulfonate, non-sea-salt sulfate, and sulfur dioxide at three sites in Canada, *Journal of Geophysical Research-Atmospheres* **101**(1996), pp. 4165-4173.

Matrai, P.A., Vernet, M., Dynamics of the vernal bloom in the marginal ice zone of the Barents Sea: Dimethyl sulfide and dimethylsulfoniopropionate budgets, *Journal of Geophysical Research-Oceans* **102**(1997), pp. 22965-22979.

McCluskey, C.S. *et al.*, A Dynamic Link between Ice Nucleating Particles Released in Nascent Sea Spray Aerosol and Oceanic Biological Activity during Two Mesocosm Experiments, *Journal of the Atmospheric Sciences* **74**(2017), pp. 151-166.

McParland, E.L., Levine, N.M., The role of differential DMSP production and community composition in predicting variability of global surface DMSP concentrations, *Limnology and Oceanography* **64**(2019), pp. 757-773.

Melin, F., Berthon, J.F., Zibordi, G., Assessment of apparent and inherent optical properties derived from SeaWiFS with field data, *Remote Sensing of Environment* **97**(2005), pp. 540-553.

Melin, F. *et al.*, Multi-sensor satellite time series of optical properties and chlorophyll-a concentration in the Adriatic Sea, *Progress in Oceanography* **91**(2011), pp. 229-244.

Middlebrook, A.M., Bahreini, R., Jimenez, J.L., Canagaratna, M.R., Evaluation of Composition-Dependent Collection Efficiencies for the Aerodyne Aerosol Mass Spectrometer using Field Data, *Aerosol Science and Technology* **46**(2012), pp. 258-271.

Mihalopoulos, N., Kerminen, V.M., Kanakidou, M., Berresheim, H., Sciare, J., Formation of particulate sulfur species (sulfate and methanesulfonate) during summer over the Eastern Mediterranean: A modelling approach, *Atmospheric Environment* **41**(2007), pp. 6860-6871.

Mihalopoulos, N., Stephanou, E., Kanakidou, M., Pilitsidis, S., Bousquet, P., Tropospheric aerosol ionic composition in the Eastern Mediterranean region, *Tellus Series B-Chemical and Physical Meteorology* **49**(1997), pp. 314-326.

Mukai, H., Yokouchi, Y., Suzuki, M., SEASONAL-VARIATION OF METHANESULFONIC-ACID IN THE ATMOSPHERE OVER THE OKI ISLANDS IN THE SEA OF JAPAN, *Atmospheric Environment* **29**(1995), pp. 1637-1648.

Navarro, G., Alvain, S., Vantrepotte, V., Huertas, I.E., Identification of dominant phytoplankton functional types in the Mediterranean Sea based on a regionalized remote sensing approach, *Remote Sensing of Environment* **152**(2014), pp. 557-575.

O'Dowd, C. *et al.*, Connecting marine productivity to sea-spray via nanoscale biological processes: Phytoplankton Dance or Death Disco?, *Scientific Reports* **5**(2015).

Orellana, M.V., Matrai, P.A., Janer, M., Rauschenberg, C.D., DIMETHYLSULFONIOPROPIONATE STORAGE IN PHAEOCYSTIS (PRYMNESIOPHYCEAE) SECRETORY VESICLES, *Journal of Phycology* **47**(2011), pp. 112-117.

Ovadnevaite, J. *et al.*, Submicron NE Atlantic marine aerosol chemical composition and abundance: Seasonal trends and air mass categorization, *Journal of Geophysical Research-Atmospheres* **119**(2014), pp. 11850-11863.

Pitarch, J., Bellacicco, M., Volpe, G., Colella, S., Santoleri, R., Use of the quasi-analytical algorithm to retrieve backscattering from in-situ data in the Mediterranean Sea, *Remote Sensing Letters* **7**(2016), pp. 591-600.

Polissar, A.V., Hopke, P.K., Harris, J.M., Source regions for atmospheric aerosol measured at Barrow, Alaska, *Environmental Science & Technology* **35**(2001), pp. 4214-4226.

Rinaldi, M. *et al.*, Primary and Secondary Organic Marine Aerosol and Oceanic Biological Activity: Recent Results and New Perspectives for Future Studies, *Advances in Meteorology*(2010).

Rinaldi, M. *et al.*, Is chlorophyll-a the best surrogate for organic matter enrichment in submicron primary marine aerosol?, *Journal of Geophysical Research-Atmospheres* **118**(2013), pp. 4964-4973.

Rinaldi, M. *et al.*, Ground level ice nucleating particles measurements at Capo Granitola, a Mediterranean coastal site, *Atmospheric Research* **219**(2019), pp. 57-64.

Rolph, G., Stein, A., Stunder, B., Real-time Environmental Applications and Display sYstem: READY, *Environmental Modelling & Software* **95**(2017), pp. 210-228.

Salgado-Hernanz, P.M., Racault, M.F., Font-Muñoz, J.S., Basterretxea, G., Trends in phytoplankton phenology in the Mediterranean Sea based on ocean-colour remote sensing, *Remote Sensing of Environment* ***221***(2019), pp. 50-64.

Sammartino, M., Di Cicco, A., Marullo, S., Santoleri, R., Spatio-temporal variability of micro-, nano- and pico-phytoplankton in the Mediterranean Sea from satellite ocean colour data of SeaWiFS, *Ocean Science* **11**(2015), pp. 759-778.

Savoie, D.L., Prospero, J.M., COMPARISON OF OCEANIC AND CONTINENTAL SOURCES OF NON-SEA-SALT SULFATE OVER THE PACIFIC-OCEAN, *Nature* **339**(1989), pp. 685-687.

Schembari, C. *et al.*, Source apportionment of PM10 in the Western Mediterranean based on observations from a cruise ship, *Atmospheric Environment* **98**(2014), pp. 510-518.

Shaw, G.E., BIO-CONTROLLED THERMOSTASIS INVOLVING THE SULFUR CYCLE, *Climatic Change* **5**(1983), pp. 297-303.

Stein, A.F. *et al.*, NOAA'S HYSPLIT ATMOSPHERIC TRANSPORT AND DISPERSION MODELING SYSTEM, *Bulletin of the American Meteorological Society* **96**(2015), pp. 2059-2077.

Toole, D.A., Siegel, D.A., Light-driven cycling of dimethylsulfide (DMS) in the Sargasso Sea: Closing the loop, *Geophysical Research Letters* **31**(2004).

Vallina, S.M., Simo, R., Strong relationship between DMS and the solar radiation dose over the global surface ocean, *Science* **315**(2007), pp. 506-508.

Volpe, G., Buongiorno Nardelli, B., Cipollini, P., Santoleri, R., Robinson, I.S., Seasonal to interannual phytoplankton response to physical processes in the Mediterranean Sea from satellite observations, *Remote Sensing of Environment* **117**(2012), pp. 223-235.

Volpe, G. *et al.*, The colour of the Mediterranean Sea: Global versus regional bio-optical algorithms evaluation and implication for satellite chlorophyll estimates, *Remote Sensing of Environment* **107**(2007), pp. 625-638.

Wang, X.F. *et al.*, Microbial Control of Sea Spray Aerosol Composition: A Tale of Two Blooms, *Acs Central Science* **1**(2015), pp. 124-131.

Watts, S.F., Brimblecombe, P., Watson, A.J., Methanesulphonic acid, dimethyl sulphoxide and dimethyl sulphone in aerosols, *Atmospheric Environment. Part A. General Topics* **24**(1990), pp. 353-359.

Westberry, T., Behrenfeld, M.J., Siegel, D.A., Boss, E., Carbon-based primary productivity modeling with vertically resolved photoacclimation, *Global Biogeochemical Cycles* **22**(2008).

Westberry, T.K., Dall'Olmo, G., Boss, E., Behrenfeld, M.J., Moutin, T., Coherence of particulate beam attenuation and backscattering coefficients in diverse open ocean environments, *Optics Express* **18**(2010), pp. 15419-15425.

Wolfe, G.V., Steinke, M., Grazing-activated production of dimethyl sulfide (DMS) by two clones of Emiliania huxleyi, *Limnology and Oceanography* **41**(1996), pp. 1151-1160.

Yoon, Y.J. *et al.*, Seasonal characteristics of the physicochemical properties of North Atlantic marine atmospheric aerosols, *Journal of Geophysical Research-Atmospheres* **112**(2007).

Zhuang, G.C., Yang, G.P., Yu, J.A., Gao, Y.A., Production of DMS and DMSP in different physiological stages and salinity conditions in two marine algae, *Chinese Journal of Oceanology and Limnology* **29**(2011), pp. 369-377.

Zorn, S.R., Drewnick, F., Schott, M., Hoffmann, T., Borrmann, S., Characterization of the South Atlantic marine boundary layer aerosol using an aerodyne aerosol mass spectrometer, *Atmospheric Chemistry and Physics* **8**(2008), pp. 4711-4728.